CONSTRUCTAL DESIGN OF A VORTEX TUBE FOR SEVERAL INLET STAGNATION PRESSURES

C. H. Marques[a],

L. A. Isoldi[a],

E. D. dos Santos[a],

and L. A. O. Rocha[b]

[a]Universidade Federal do Rio Grande

FURG, Escola de Engenharia, Av. Itália, km 8,

CEP: 96201-090, CP 474, Rio Grande, RS,

Brasil, cristoferhood@gmail.com

[b]Universidade Federal do Rio Grande do Sul

UFRGS, Departamento de Engenharia

Mecânica, UFRGS, Rua Sarmento Leite, 425,

CEP: 90050-170, Porto Alegre, RS, Brasil.

ABSTRACT

The present paper shows a numerical study concerned with the geometrical optimization of a vortex tube device by means of Constructal Design for several inlet stagnation pressures. In the present study, it is evaluated a vortex tube with two-dimensional axisymmetric computational domain with dry air as the working fluid. The compressible and turbulent flows are numerically solved with the commercial CFD package FLUENT, which is based on the Finite Volume Method. The turbulence is tackled with the k-ε model into the Reynolds Averaged Navier-Stokes (RANS) approach. The geometry has one global restriction, the total volume of the cylindrical tube, and four degrees of freedom: d_3/D (the ratio between the diameter of the cold outlet and the diameter of the vortex tube), d_1/D (the ratio between the diameter of the inlet nozzle and the diameter of the vortex tube), L_2/L (the ratio between the length of the hot exit annulus and the length of the vortex tube) and D/L (the ratio between the diameter of the vortex tube and its length). The degree of freedom L_2/L will be represented here by the cold mass fraction (y_c). In the present work it is optimized the degrees of freedom y_c and d_3/D while the other degrees of freedom and the global restriction are kept fixed. The purpose here is to maximize the amount of energy extracted from the cold region (cooling effect) for several geometries, as well as, investigate the influence of the inlet stagnation pressure over the optimal geometries. Results showed an increase of the twice maximized cooling heat transfer rate of nearly 330 % from 300 kPa to 700 kPa. Moreover, the optimization showed a higher dependence of $(d_3/D)_o$ for the lower range of inlet pressures, while the optimization is more dependent of $y_{c,oo}$ for higher inlet stagnation pressures.

Keywords: constructal design, optimization, vortex tube, numerical study.

NOMENCLATURE

A	Area, m^2
D	diameter of the vortex tube, m
d_1	diameter of inlet nozzle, m
d_3	diameter of cold outlet, m
k	thermal conductivity, W/(m·K)
L	length of vortex tube, m
L_2	length of the outlet exit, m
m	mass flow rate, (kg/s)
m_c	cold mass flow rate, (kg/s)
p	pressure, kPa
Pr	Prandtl number
Q_c	cold heat transfer rate, W
T	temperature, K
t	temporal domain, s
V	volume, m^3
v	velocity, (m/s)
y_c	cold mass fraction

Greek symbols

α	tangential angle, degree
α	thermal diffusivity, (m^2/s)
α_t	turbulent thermal diffusivity, (m^2/s)
ε	dissipation rate, (m^2/s^3)
κ	turbulent kinetic energy, (m^2/s^2)
μ	dynamical viscosity, kg/(m·s)

μ_t	turbulent dynamical viscosity, kg/(m·s)
ρ	density, kg/m^3
υ	kinematic viscosity, m^2/s
Ω	spatial domain, m
ΔT_C	cold air temperature drop, K
ΔT_H	hot air temperature drop, K

Subscripts

t	turbulent
m	maximum cold heat transfer rate
mm	twice maximized cold heat transfer rate
o	optimal
oo	twice optimized
C	cold exit
H	hot exit

Superscripts

(¯)	time-averaged variables (RANS)

INTRODUCTION

The vortex tube (also known as Ranque-Hilsch vortex tube) is a mechanical device which splits a compressed high-pressure gas stream into cold and hot lower pressure streams without any chemical

reactions or external energy supply (Ranque, 1934; Hilsch, 1947; Eiamsa-ard and Promvonge, 2008). Such a separation of the flow into regions of low and high total temperature is referred to as the temperature (or energy) separation effect. The device consists of a simple circular tube, one or more tangential nozzles, and a throttle valve. Figure 1 depicts schematically two types of vortex tube: counter flow (Fig. 1a) and parallel flow (Fig. 1b). The operational principle of a counter flow vortex tube, which is the scope of the present work, Fig. 1a, consists of a high pressure gas that enters the vortex tube and passes through the nozzle(s). The gas expands through the nozzle and achieves a high angular velocity, causing a vortex-type flow in the tube. There are two exits to the tube: the hot exit is placed near the outer radius of the tube at the end away from the nozzle and the cold exit is placed at the center of the tube at the same end as the nozzle.

By adjusting a throttle valve (cone valve) downstream of the hot exit it is possible to vary the fraction of the incoming flow that leaves through the cold exit, referred as cold fraction. This adjustment affects the amount of cold and hot energy that leaves the vortex tube in the device exits.
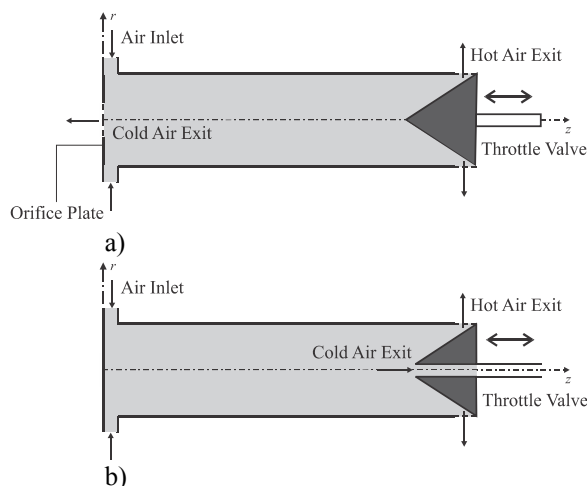

Figure 1. Operating principle of two types of vortex tubes: (a) counter flow and (b) parallel flow.

The vortex tube has been subject of studies due to its enormous applications in engineering, such as to cool parts of machines, refrigeration, cool electric or electronic control cabinets, cooling of equipments in laboratories dealing with explosive chemicals, chill environmental chambers, cool foods, liquefaction of natural gas and cooling suits (Eiamsa-ard and Promvonge, 2008; Fin' ko, 1984; Bruno, 1993; Kirmaci, 2009; Dutta et al., 2010). Moreover, the lack of moving parts, electricity and others advantages make the device attractive for a number of specialized applications where simplicity, robustness, reliability and general safety are desired (Lewis and Bejan, 1999). Other important motivation for the study of vortex tube is concerned with the complexity of the energy separation phenomenon in the compressible and turbulent flow.

In this sense, several studies have been performed to explain the phenomena occurring during the energy separation inside the vortex tube (Lewis and Bejan, 1999; Harnett and Eckert, 1957; Stephan et al., 1983). Computational fluid dynamics (CFD) modeling has also been utilized to improve the comprehension about the energy separation. The most recent works has investigating the energy separation effect using several turbulence models. For instance, Aljuwayhel et al. (2005) investigated the energy separation mechanism using the commercial code FLUENT, based on the finite volume method (FVM). They observed that the standard $k - \varepsilon$ turbulence model predicted the velocity and temperature separation better than the RNG $k - \varepsilon$ turbulence model. Dutta et al. (2010) studied the influence of different Reynolds Averaged Navier-Stokes (RANS) turbulence models: standard $k - \varepsilon$, RNG $k - \varepsilon$, standard $k - \omega$ and SST $k - \omega$. A comparison of the temperature separation obtained numerically and experimentally corroborates the previous findings of Aljuwayhel et al. (2005). Farouk and Farouk (2007) used large eddy simulation (LES) and compared with previous experimental results of Skye et al. (2006) and $k - \varepsilon$ predictions. The authors noticed that temperature separation predicted with LES was closer to the experimental results in comparison with those reached with RANS model. It is worth mention that the computational effort for LES is, in general, several times higher than that observed for RANS simulations. This fact prevents the use of LES for optimization studies, since several simulations are required.

Concerning the optimization of the vortex tube, according to Eiamsa-ard and Promvonge (2008) two important parameters must be taken into account. The first is the geometrical characteristics of the vortex tube (diameter and length of the hot and cold tubes, the diameter of the cold orifice, shape of the hot tube, number of inlet nozzles and others). The second is focused on the thermo-physical parameters such as inlet gas pressure, cold mass fraction (ratio between the mass coming out the cold exit and the mass that enters) and type of gas (air, oxygen, helium and methane). Studies in this subject have been presented in literature. For example, Promvonge and Eiamsa-ard (2005) reported the effects of the number of inlet tangential nozzles, the cold orifice diameter and the tube insulations on the temperature reduction and isentropic efficiency of the vortex tube. Aydin and Baki (2006) investigated experimentally the energy separation in a counter flow vortex tube having various geometrical and thermo-physical parameters. Pinar et al. (2009) investigated the effects of inlet pressure, nozzle number and fluid type factors on the tube vortex performance by means of Taguchi method. However, it has not been presented studies concerned with the geometric optimization of the

vortex tube by means of constructal design (Bejan, 2000; Bejan and Lorente, 2008; Bejan and Zane, 2012), with exception of the works of Marques et al. (2011) and Dos Santos et al. (2012), which optimized the degrees of freedom y_c and d_3/D for one inlet stagnation pressure of $p_{01} = 700$ kPa.

In the present work it is considered the design optimization of a vortex tube device by means of constructal design and for several inlet stagnation pressures ($p_{01} = 300$ kPa, 500 kPa and 700 kPa). It is evaluated a vortex tube with axisymmetric computational domain. The compressible and turbulent flow of dry air is numerically solved with a commercial CFD package based on the Finite Volume Method, FLUENT (2007). The turbulence is tackled with the standard $k - \varepsilon$ model into the Reynolds Averaged Navier-Stokes (RANS) approach. The geometry evaluated here has one global restriction, the total volume of the cylindrical tube, and four degrees of freedom: d_3/D (the ratio between the diameter of the cold outlet and the diameter of the vortex tube, cold orifice ratio), d_1/D (the ratio between the nozzle diameter of the air entering and the diameter of the vortex tube), y_c (cold mass fraction, L_2/L) and D/L (the ratio between the diameter of the vortex tube and its length). The purpose here is to maximize the amount of energy extracted from the cold region (cooling effect) for several geometries. Moreover, all evaluated geometries are simulated for several ratios between the fixed inlet stagnation pressure (p_{01}) and the static pressure of the hot exit (p_2), evaluating the influence of the former parameter over the optimal shapes of the vortex tube. In the present work it is optimized the degrees of freedom d_3/D and y_c while the other degrees of freedom are kept fixed.

MATHEMATICAL MODEL

The analyzed physical problem consists of a two dimensional axisymmetric cylindrical cavity, as illustrated in Fig. 2. The dry air entering the tube is modeled as an ideal gas with constant specific heat capacity, thermal conductivity, and viscosity. The inlet stagnation conditions are fixed at $p_{01} = 300$ kPa and $T_{01} = 300$ K for the verification case. For the optimization cases the inlet stagnation pressures are varied ($p_{01} = 300$ kPa, 500 kPa and 700 kPa). The intake air enters with an angle of $\alpha = 9^\circ$ with respect to tangential direction. The static pressure at the cold exit boundary (p_3) is fixed at atmospheric pressure. For the hot exit boundary, several simulations are performed with various pressures (p_2) in order to simulate the effect of throttle valve. For each fixed pressure, one specific value of cold mass fraction ($y_c = m_c/m$) is reached. Once it is considered a two dimensional axisymmetric domain an axis is imposed in the lower surface of the domain, Fig. 2. The other surfaces present the no-slip and adiabatic conditions. Moreover, the following dimensions are assumed: L

$= 1.0 \times 10^{-1}$ m, $L_2 = 1.5 \times 10^{-3}$ m, $D = 2 \times 10^{-2}$ m, $d_1 = 1.0 \times 10^{-3}$ m. For the verification case, $d_3 = 6.0 \times 10^{-3}$ m. For the optimization study, the objective of the analysis is to determine the optimal geometry (d_3/D, d_1/D, L_2/L and D/L) that leads to the maximum cooling heat transfer rate (Q_c). In the present work, it is optimized the degree of freedom d_3/D while the other degrees of freedom are assumed fixed: $d_1/D = 0.05$, $L_2/L = 0.015$ and $D/L = 0.2$.
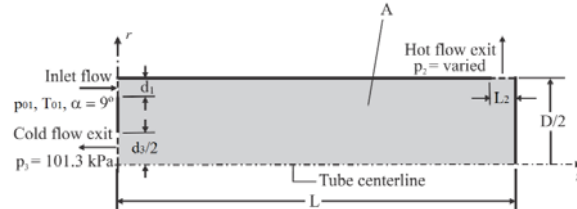

Figure 2. Domain of the vortex tube.

According to constructal design (Bejan and Lorente, 2008) the optimization can be subjected to the total volume constraint,

$$V = \frac{\pi D^2}{4} L \qquad (1)$$

For all evaluated cases, it is solved the time-averaged conservation equations of mass, momentum and energy, as well as, the state equation for the turbulent flow, which is given respectively by (Wilcox, 2002; Launder and Spalding, 1972; Hinze, 1975; Bejan, 2004):

$$\frac{\partial \overline{\rho}}{\partial t} + \frac{\partial}{\partial x_i}\left(\overline{\rho}\,\overline{u_i}\right) = 0 \qquad (2)$$

$$\frac{\partial}{\partial t}\left(\overline{\rho u_i}\right) + \frac{\partial}{\partial x_i}\left(\overline{\rho u_i u_j}\right) = -\frac{\partial \overline{p}}{\partial x_j} +$$
$$\frac{\partial}{\partial x_j}\left[\mu\left(\frac{\partial \overline{u_i}}{\partial x_j} + \frac{\partial \overline{u_j}}{\partial x_i} - \frac{2}{3}\delta_{ij}\frac{\partial \overline{u_k}}{\partial x_k}\right)\right] + \frac{\partial}{\partial x_j}\left(-\overline{\rho u_i' u_j'}\right) \quad (3)$$

$$\frac{\partial}{\partial t}\left(\overline{\rho E}\right) + \frac{\partial}{\partial x_i}\left[\overline{u_i}\left(\overline{\rho E} + \overline{p}\right)\right] = -\frac{\partial}{\partial x_j}\left[k\frac{\partial T}{\partial x_j} - q_j'\right]$$
$$- \frac{\partial\left[\overline{u_i}\left(\overline{\tau_{ij}}\right)_{eff}\right]}{\partial x_j} + S_h \qquad (4)$$

$$\overline{p} = \overline{\rho} R \overline{T} \qquad (5)$$

where $(\overline{})$ represents the time-averaged variables, $()'$ represents the floating parts of the variables; the

indices i, j and k can assume the values 1, 2 or 3 representing the directions in space; E is the total energy (J/kg); q'_j represents the energy flux as heat due to turbulence (W/m^2);$(\tau_{ij})_{eff}$ is known as turbulent tensor (Pa); R is the gas constant (J/(kg·K)); S_h is the source term of energy equation (W/m^3); t represents the time domain (s); ρ is the density of the fluid (kg/m^3), μ is the dynamical viscosity (kg/(m·s)), k is the thermal conductivity of the fluid (W/m·K)), u is the velocity (m/s), p is the pressure (Pa), T is the temperature (K), δ_{ij} is the Kronecker delta.

The last term for Eq. (3) is the Reynolds tensor and can be defined by the Boussinesq hypothesis as (Wilcox, 2002; Launder and Spalding, 1972):

$$-\overline{\rho u_i' u_j'} = \mu_t\left(\frac{\partial \overline{u_i}}{\partial x_j} + \frac{\partial \overline{u_j}}{\partial x_i}\right) - \frac{2}{3}\left(\rho k + \mu_t \frac{\partial \overline{u_k}}{\partial x_k}\right)\delta_{ij} \quad (6)$$

where μ_t is turbulent viscosity (kg/(m·s)) and k is the turbulent kinetic energy (J/kg).

The turbulent heat flux that appears in Eq. (4) is defined by (Wilcox, 2002):

$$-q'_j = k_t \frac{\partial \overline{T}}{\partial x_j} \quad (7)$$

where k_t is the turbulent thermal conductivity (W/(m·K)).

The turbulent deformation tensor, $(\tau_{ij})_{eff}$, is given by (Wilcox, 2002):

$$\left(\tau_{ij}\right)_{eff} = \mu_{eff}\left(\frac{\partial \overline{u_i}}{\partial x_j} + \frac{\partial \overline{u_j}}{\partial x_i}\right) - \frac{2}{3}\delta_{ij}\mu_{eff}\frac{\partial \overline{u_k}}{\partial x_k} \quad (8)$$

where μ_{eff} is the effective viscosity (kg/(m·s)).

The time-averaged fields of velocity, pressure and temperature are reached by means of standard $k - \varepsilon$ model (Wilcox, 2002; Launder and Spalding, 1972). According to this model it is required the solution of two additional equations for the turbulent kinetic energy k and its dissipation rate ε, which can be expressed as follows:

$$\frac{\partial}{\partial t}\left(\overline{\rho}k\right) + \frac{\partial}{\partial x_i}\left(\overline{\rho}k\overline{u_i}\right) = -\frac{\partial}{\partial x_j}\left[\left(\mu + \frac{\mu_t}{\sigma_k}\right)\frac{\partial k}{\partial x_j}\right] + \\ G_k + G_b - \overline{\rho}\varepsilon - Y_M + S_k \quad (9)$$

$$\frac{\partial}{\partial t}\left(\overline{\rho}\varepsilon\right) + \frac{\partial}{\partial x_i}\left(\overline{\rho}\varepsilon\overline{u_i}\right) = -\frac{\partial}{\partial x_j}\left[\left(\mu + \frac{\mu_t}{\sigma_\varepsilon}\right)\frac{\partial \varepsilon}{\partial x_j}\right] + \\ C_{1\varepsilon}\frac{\varepsilon}{k}\left(G_k + C_{3\varepsilon}G_b\right) - C_{2\varepsilon}\overline{\rho}\frac{\varepsilon^2}{k} + S_\varepsilon \quad (10)$$

For Eq. (9) and Eq. (10) G_k represents the generation of turbulent kinetic energy due to the time-averaged velocity gradientes (W/m^3); G_b is the generation of turbulent kinetic energy due to buoyancy forces (W/m^3) (which in the present study is considered null); S_k and S_ε are sources of turbulent kinetic energy and dissipation rate (W/m^3), respectively; C_μ, $C_{1\varepsilon}$, $C_{2\varepsilon}$ and $C_{3\varepsilon}$ are constants; σ_k and σ_ε are turbulent Prandtl numbers for the equations of k and ε. The latter constants, with exception of $C_{3\varepsilon} = 0$, defined for the standard $k - \varepsilon$ model can be seen in Tab. 1 (Wilcox, 2002).

Table 1. Model constants appearing in the governing equations.

C_μ	$C_{\varepsilon 1}$	$C_{\varepsilon 2}$	σ_k	σ_ε	Pr_t
0.09	1.44	1.92	1.0	1.3	0.85

In order to calculate turbulence quantities accurately in the near-wall region, it is employed standard wall functions for velocity and temperature fields (Launder and Spalding, 1972).

The cooling heat transfer rate (Q_c) is evaluated as following:

$$Q_c = m_c c_p\left(T_{01} - T_{03}\right) \quad (11)$$

where m_c represents the mass flow rate of air leaving the device by cold output; c_p represents the specific heat capacity of the air; T_{01} and T_{03} represents the total temperature of the air in the inlet and in the cold outlet, respectively.

NUMERICAL MODEL

Concerning the simulation of compressible turbulent flows, from Eq. (2) until Eq. (5) are solved by using a CFD package based on rectangular finite volume method (FLUENT, 2007). The solver is density based and all simulations were performed with the second-order upwind advection scheme. More details concerned with the finite volume method can be found in Patankar (1980) and Versteeg and Malalasekera (2007).

The spatial discretization is performed with rectangular finite volumes using the software GAMBIT. The grid is more refined for the highest velocity and temperature gradients regions. The grid is refined several times until the achievement of the criterion $|(T_{0\,min}^{j} - T_{0\,min}^{j+1})/T_{0\,min}^{j}| < 5 \times 10^{-4}$ in order to reach the independent grid. $T_{0\,min}^{j}$ represents the minimal total temperature along the domain for the actual grid and $T_{0\,min}^{j+1}$ corresponds to the minimal total temperature for the following grid. Moreover, for each refinement the number of volumes is increased approximately two times. The grid sensibility study for the verification case is presented in Marques et al. (2011) and Dos Santos et al. (2012).

The independent grid was obtained with 11760 volumes. The verification and validation of the code was also performed in Marques et al. (2011) and Dos Santos et al. (2012) and, for the sake of brevity, will not be reproduced here.

RESULTS AND DICUSIONS

An One example of one level of optimization is shown in Fig. 3. In this graph it is depicted the effect of the cold mass fraction (y_c) over the cooling heat transfer rate (Q_c) for several ratios of d_3/D. As observed in the previous studies of Marques et al. (2011) and Dos Santos et al. (2012), which evaluated the geometries for $p_{01} = 700$ kPa only, one optimal intermediate value of y_c is reached for each curve of d_3/D. In the present work similar behavior was found for several inlet stagnation pressures evaluated $p_{01} = 300$ kPa, 500 kPa and 700 kPa. The best shapes obtained in Fig. 3 are compiled in Fig. 4. For $p_{01} = 700$ kPa, it is possible to observe one optimal ratio of $(d_3/D)_o = 0.43$, which conducts to a second maximization of the once maximized cooling heat transfer rate ($Q_{c,m}$), $Q_{c,mm} = 267.59$ W. Moreover, the best cold mass fractions $y_{c,o}$ has the same tendency observed for the cooling heat transfer rate ($Q_{c,m}$). Nonetheless, the ratio of d_3/D that lead to the highest value of $y_{c,o}$ is not the same that lead to the maximum $Q_{c,m}$.
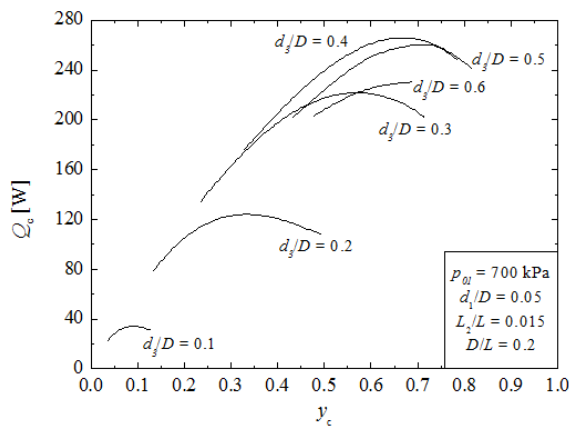

Figure 3. The effect of the cold mass fraction (y_c) over the cooling heat transfer rate (Q_c) for several ratios of d_3/D.

Figure 5 shows the effect of the ratio between the diameter of the cold outlet and the vortex tube diameter (d_3/D) over cold mass flow rate for the optimal shape ($m_{c,o}$) and over the once optimized specific cooling heat transfer rate ($Q_c/m_c)_o$. It can be observed an increase of the cold mass flow rate for once optimized shape until a highest value of $m_{c,o} = 1.24 \times 10^{-2}$ kg/s, which is noticed for $d_3/D = 0.49$. For the specific cooling heat transfer rate ($Q_c/m_c)_o$ as a function of the ratio (d_3/D), it is seen a decrease of

the former variable in the range ($0.1 \leq d_3/D \leq 0.18$). It is also observed a maximum value of ($Q_c/m_c)_o = 22685$ J/kg for $d_3/D = 0.33$. For $d_3/D \geq 0.33$, the values of ($Q_c/m_c)_o$ decreases again. The values of ($Q_c/m_c)_o$ for $d_3/D = 0.1$, 0.18 and 0.6 are 3.3 %, 5.2 % and 13.7 % lower than that found for the maximum value of ($Q_c/m_c)_o$. Other important observation is that the optimal ratio ($d_3/D)_o = 0.43$, which lead to the twice maximized cold heat transfer rate ($Q_{c,mm}$), is not the same one that conducts to the highest $m_{c,o}$, ($d_3/D = 0.49$) nor that one which lead to the highest ($Q_c/m_c)_o$, ($d_3/D = 0.33$). In other words, the maximum cooling heat transfer rate ($Q_{c,mm}$) is a result of the product between the twice optimized cold mass flow rate and the specific cold heat transfer rate, which for ($d_3/D)_o = 0.43$ are $m_{c,oo} = 1.21 \times 10^{-2}$ kg/s ($Q_c/m_c)_{oo} = 22200$ J/kg, respectively.
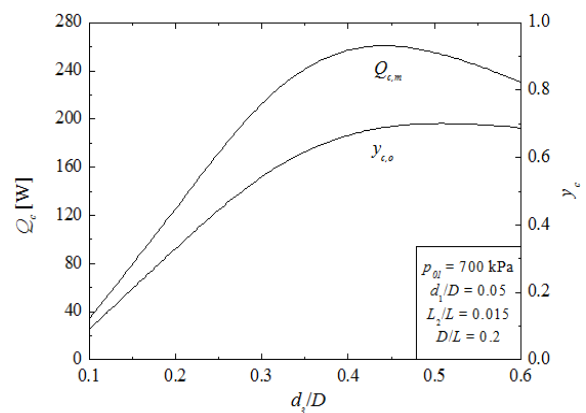

Figure 4. The first optimization of the cooling heat transfer rate (Q_c) and the optimal cold mass fraction (y_c) as function of d_3/D.
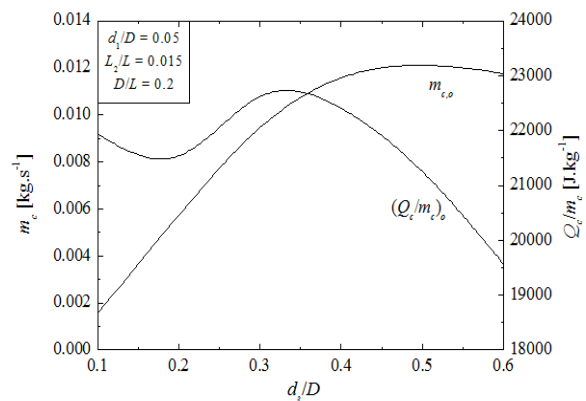

Figure 5. The effect of the degree of freedom d_3/D over the cold mass flow rate for the optimal shapes ($m_{c,o}$) and the once maximized specific cooling heat transfer rate ($Q_c/m_c)_m$.

Figure 6 shows the effect of the inlet stagnation pressure (p_{01}) over the twice maximized cooling heat transfer rate ($Q_{c,mm}$), as well as, over the once optimized ratio ($d_3/D)_o$ and twice optimized cold

mass fraction ($y_{c,oo}$). For the evaluated range of 300 kPa $\leq p_{01} \leq$ 700 kPa, it is noticed an increase almost linear of the twice maximized cooling heat transfer rate ($Q_{c,mm}$) with the increase of the inlet pressure (p_{01}). For p_{01} = 700 kPa, the twice maximized cooling heat transfer rate $Q_{c,mm}$ = 267.59 W is nearly 330 % higher than the value found for the inlet stagnation pressure of p_{01} = 300 kPa. Regarding the optimal shapes of the vortex tube, for the range of 300 kPa $\leq p_{01} \leq$ 400 kPa, the twice optimized cold mass fraction is almost constant. For higher values of p_{01}, it is observed an increase of $y_{c,oo}$ as a function of p_{01}, i.e., for a real system this effect would represent the closing of the valve. For the degree of freedom ($d_3/D)_o$ it is shown an increase from ($d_3/D)_o$ = 0.41 to ($d_3/D)_o$ = 0.43 for pressures of p_{01} = 300 kPa and p_{01} = 700 kPa, respectively. It is also observed an stabilization of the once optimized ratio between the diameter of the cold outlet and the diameter of the vortex tube of ($d_3/D)_o$ = 0.43 for inlet pressures higher than $p_{01} \geq$ 500 kPa. To summarize, it is possible to state that the optimization is more dependent of ($d_3/D)_o$ for the lower range of inlet pressures, while the optimization is more dependent of $y_{c,oo}$ for higher inlet stagnation pressures.
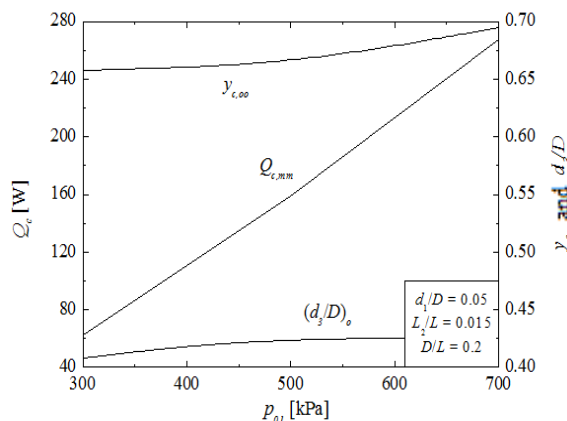

Figure 6. Effect of the inlet stagnation pressure (p_{01}) over the twice maximized cooling heat transfer rate ($Q_{c,mm}$) and over the optimized degrees of freedom ($d_3/D)_o$ and ($y_{c,oo}$).

Figure 7 shows the variation of total temperatures of hot and cold exits ($T_{0h,oo}$ and $T_{0c,oo}$) for the twice optimized shape as a function of the inlet stagnation pressure (p_{01}). It is seen an almost linear increase of $T_{0h,oo}$ from $T_{0h,oo}$ = 321 K to $T_{0h,oo}$ = 350 K for the pressures of p_{01} = 300 kPa and p_{01} = 700 kPa, respectively, i.e., a difference of 8.3 %. On the opposite, $T_{0c,oo}$ decreases smoothly from $T_{0c,oo}$ = 289 K to $T_{0c,oo}$ = 278 K for the pressures of p_{01} = 300 kPa and p_{01} = 700 kPa, i.e., a reduction of nearly 4.0 %. Moreover, it is noticed that the difference between the total temperatures of the hot and cold exits ($\Delta T_{0,oo}$) increases from 32 K to 72 K, for the pressures of p_{01} = 300 kPa and p_{01} = 700 kPa, respectively.

Figure 8 shows the effect of the inlet stagnation pressure (p_{01}) over the twice optimized specific cooling heat transfer rate ($Q_c/m_c)_{oo}$ and over the twice optimized mass flow rate ($m_{c,oo}$). As previously observed for the twice maximized cooling heat transfer rate ($Q_{c,mm}$), there is not one intermediate optimal point. In other words, the highest value of ($Q_c/m_c)_{oo}$ is achieved for the highest pressure, p_{01} = 700 kPa. It is also observed an increase of the ($Q_c/m_c)_{oo}$ from ($Q_c/m_c)_{oo}$ = 11405 J/kg (for p_{01} = 300 kPa) to ($Q_c/m_c)_{oo}$ = 22200 J/kg (for p_{01} = 700 kPa), which represents a difference of 94.7 %. For $m_{c,oo}$ it is noticed an increase almost linear from $m_{c,oo}$ = 5.48 × 10^{-3} kg/s (for p_{01} = 300 kPa) to $m_{c,oo}$ = 1.21 × 10^{-2} kg/s (for p_{01} = 700 kPa), i.e., an increase of nearly 121 %.
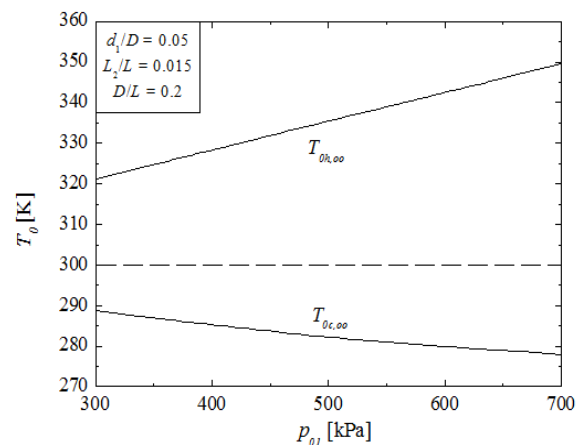

Figure 7. Effect of the inlet pressure (p_{01}) over the total temperatures of hot and cold exits ($T_{0h,oo}$ and $T_{0c,oo}$) for the twice optimized shape.
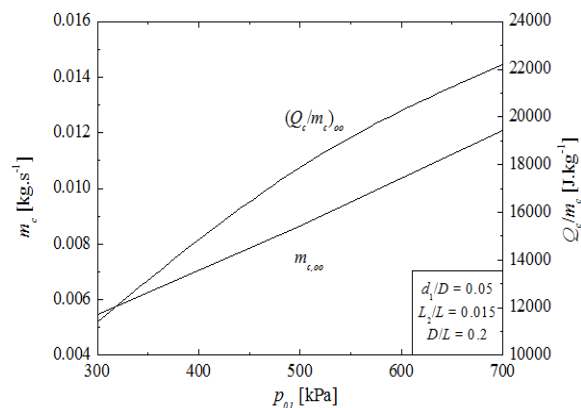

Figure 8. Effect of the inlet stagnation pressure (p_{01}) over the twice maximized ($Q_c/m_c)_{mm}$ and over the twice optimized cold mass flow rate ($m_{c,oo}$).

CONCLUSIONS

In the present work it was considered the numerical study of design optimization of a vortex tube device by means of constructal design. It was evaluated a vortex tube with axisymmetric

computational domain. The compressible and turbulent flow of dry air was numerically solved with a commercial CFD package based on the Finite Volume Method, FLUENT (2007). The turbulence was tackled with the standard $k - \varepsilon$ model into the Reynolds Averaged Navier-Stokes (RANS) approach. In this study it was optimized the degrees of freedom d_3/D (the ratio between the diameter of the cold outlet and the diameter of the vortex tube) and cold mass fractions (y_c) for several inlet stagnation pressures (300 kPa $\leq p_{01} \leq$ 700 kPa) similarly to the study performed in Marques et al. (2011) and Dos Santos (2012) which optimized the shape for p_{01} = 700 kPa. The other degrees of freedom (d_1/D, L_2/L and D/L) were kept fixed.

It was investigated the effect of the cold mass fraction (y_c) over the cold heat transfer rate (Q_c) for several fixed ratios of d_3/D. In general, it was observed one optimal ratio $y_{c,o}$ that led to the maximum heat transfer rate ($Q_{c,m}$), except for the highest evaluated ratio d_3/D = 0.6. Moreover, it was observed that the optimal ratio $(d_3/D)_o$, which lead to the twice maximized cold heat transfer rate ($Q_{c,mm}$), was not the same one that conducted to the highest $m_{c,o}$ nor that one which lead to the highest $(Q_c/m_c)_o$. The same behavior was noticed for the several inlet stagnation pressures simulated in this study.

As previously observed in the studies of Marques et al. (2011) and Dos Santos et al. (2012), twice optimized $y_{c,oo}$ and once optimized $(d_3/D)_o$ presented the same behavior for the several pressures evaluated, p_{01} = 300 kPa, 500 kPa and 700 kPa. The results also shown an increase of the twice maximized cooling heat transfer rate ($Q_{c,mm}$) of approximately 330 % from p_{01} = 300 kPa to p_{01} = 700 kPa. Moreover, the optimization of the cooling heat transfer was more dependent of $(d_3/D)_o$ for the lower range of inlet pressures, while the optimization was more dependent of $y_{c,oo}$ for higher inlet stagnation pressures.

To summarize, the present work provided a theoretical recommendation about the best geometrical configurations by means of Constructal Design for a vortex tube operating with compressed turbulent flow of dry air, with fixed ratios of d_1/D = 0.05 and D/L = 0.2 and for several inlet stagnation pressures (300 kPa $\leq p_{01} \leq$ 700 kPa), which represents various operating regimes.

ACKNOWLEDGMENT

REFERENCES

Aljuwayhel, N. F., Nellis, G. F., 2005, and Klein, S. A., Parametric and Internal Study of the Vortex Tube Using a CFD Model, International Journal of Refrigeration, Vol. 28, pp. 442-450.

Aydin, O., and Baki, M., 2006, An Experimental Study on the Design Parameters of a Counter Flow Vortex Tube, *Energy*, Vol. 31 (14), pp. 2763-2772.

Bejan, A., 2000, *Shape and Structure, from Engineering to Nature*, Cambridge University Press, UK.

Bejan, A., 2004, *Convection Heat Transfer*, John Wiley, Durham, USA.

Bejan, A., and Lorente, S., 2008, *Design with Constructal Theory*, John Wiley and Sons Inc.

Bejan, A., and Zane, P., 2012, *Design in Nature*, 1st ed., Doubleday.

Bruno, T. J., 1993, Applications of the Vortex Tube in Chemical Analysis Part I: Introductory Principle, American Laboratory, Vol. 25, pp. 15-20.

Dos Santos, E. D., Marques, C. H., Stanescu, G., Isoldi, L. A., and Rocha, L. A. O., 2012, Constructal Design of Vortex Tubes (Chapter 15). In: L. A. O. Rocha, S. Lorente and A. Bejan (Eds). *Constructal Law and the Unifying Principle of Design*, Springer.

Dutta, T., Sinhamahapatra, K. P., and Bandyopdhyay, S. S., 2010, Comparison of different Turbulence Models in Predicting the Temperature Separation in a Ranque-Hilsch Vortex Tube, International Journal of Refrigeration, Vol. 33 (4), pp. 783-792.

Eiamsa-ard, S., and Promvonge, P., 2008, Review of Ranque-Hilsch Effects in Vortex Tubes, Renewable and Sustainable Energy Reviews, Vol. 12, pp. 1822-1842.

Farouk, T., and Farouk, B., 2007, Large Eddy Simulations of the Flow Field and Temperature Separation in the Ranque-Hilsch Vortex Tube, International Journal of Heat and Mass Transfer, Vol. 50, pp. 4724-4735.

Fin' ko, V. E., 1984, Cooling and Condensation of a Gas in a Vortex Flow, Soviet Phys: Tech Phys., Vol. 28 (9), pp. 1089 - 1093.

FLUENT , 2007, ANSYS (version 6.3.16), Inc.

Harnett, J. P., and Eckert, E. R. G., 1957, Experimental Study of the Velocity and Temperature Distribution in a High-Velocity Vortex-Type Flow, *Transactions of the ASME*, Vol. 79 (4), pp. 751-758.

Hilsch, R., 1947, The Use of the Expansion of Gases in a Centrifugal Field as a Cooling Process, Review Science Instruments, Vol. 18, pp. 108-113.

Hinze, J. O., 1975, *Turbulence*, McGraw-Hill, New York, USA.

Kirmaci, V., 2009, Exergy Analysis and Performance of a Counter Flow Ranque-Hilsch Vortex Tube Having Various Nozzle Numbers at Different Inlet Pressures of Oxygen and Air,

International Journal Refrigeration, Vol. 32, pp. 1626-1633.

Launder, B. E., and Spalding, D. B., 1972, *Lectures in Mathematical Models of Turbulence*, London, Academic Press.

Lewis, J., and Bejan, A., 1999, Vortex Tube Optimization Theory, Energy, Vol. 24, pp. 931-943.

Marques, C. H., Stanescu, G., Isoldi, L. A., Dos Santos, E. D., and Rocha, L. A. O., 2011, Constructal Design of a Vortex Tube, in: *V Constructal Law Conference*, Vol. 1, pp. 1-8.

Patankar, S. V., 1980, *Numerical Heat Transfer and Fluid Flow*, McGraw-Hill, New York, USA.

Pinar, A. M., Uluer, O., and Kirmaci, V., 2009, Optimization of Conter Flow Ranque-Hilsch Vortex Tube Performance Using Taguchi Method, International Journal of Refrigeration, Vol. 32 (6), pp. 1487-1494.

Promvonge, P., and Eiamsa-ard, S., 2005, Investigation on the Vortex Termal Separation in a Vortex Tube Refrigerator, ScienceAsia, Vol. 31 (3), pp. 215-223.

Ranque, G. J., 1934, Expériences sur la Détente Giratoire Avec Productions Simultanées d'um Échappement d'air Chaud et d'um Échappement d'air Froid, Journal of Physique Radium, 4:112S – 5S, 1933, United States Patent No. 1,952,281.

Skye, H. M., Nellis, G. F., and Klein, S. A., 2006, Comparison of CFD Analysis to Empirical Data in a Commercial Vortex Tube, International Journal of Refrigeration, Vol. 29, pp. 71-80.

Stephan, K., Lin, S., Durst, M., Huang, F., and Seher, D., 1983, An investigation of Energy Separation in a Vortex Tube*,* International Journal Heat and Mass Transfer, Vol. 26 (3), pp. 341-348.

Versteeg, H. K., and Malalasekera, W., 2007, *An Introduction to Computational Fluid Dynamics – The Finite Volume Method*, Pearson, England.

Wilcox, D. C., 2002, *Turbulence Modeling for CFD*, DCW Industries, La Canada, USA.